Viser Technology Pte. Ltd.
Research and Application of Materials Science
https://doi.org/10.33142/msra.v1i1.668

Research Article Open Access

Construction of MnO_2 Nanowire for a High-Performance Lithium Ion Supercapacitor

Wenbo Wang[1], Yanhong Shi[1], Yang Su[1], Yihai Wang[1], Haizhu Sun[1*]

[1] National & Local United Engineering Laboratory for Power Battery, College of Chemistry, Northeast Normal University, Changchun, China

***Corresponding Author:** Haizhu Sun, 5268 Renmin Street, Changchun, 130024, China; sunhz335@nenu.edu.cn*

Abstract:
Developing lithium ion capacitors possessing both brilliant energy and power density is still significant for numerous re-searchers. In this paper, we synthesized MnO_2 nanowires via a simple hydrothermal process. The nanostructure MnO_2 can expose more electrochemical sites and thus optimize the kinetics of Li^+. Moreover, we used MnO_2 nanowires (MnO_2 NWs) as anode and a N-doped porous carbon (NPC) as cathode to assemble lithium ion capacitors (MnO_2 NWs//NPC LIC). Compared to the traditional supercapacitor with aqueous electrolyte, the MnO_2 NWs//NPC LIC exhibits a wider voltage of 0-4.2 V, which is helpful to enhance its energy and power density. Furthermore, MnO_2 NWs//NPC LIC can deliver an excellent capacity of 150 mAh g^{-1} with an excellent energy density of 82.7 Wh kg^{-1} and power density of 1.05 kW kg^{-1}. Meanwhile, a good cyclic stability of LICs with a 20% retention after 1000 times charge and discharge process proves its practical potential, indicating a good promising for the application in storage devices.

Keywords: *Manganese dioxide; Nanostructure; N-doped porous carbon; Lithium-ion supercapacitor*

Citation: W. B. Wang, et al., Construction of MnO_2 Nanowire for a High-Performance Lithium Ion Supercapacitor. *Res Appl Mat Sci*, 2019,1(1): 18-23. https://doi.org/10.33142/msra.v1i1.668

1. Introduction

The uninterrupted consumption of fossil fuel cells for huge energy supply boosts the rapid development of energy storage devices [1, 2]. Compared to other energy storage devices [3], lithium ion batteries (LIBs) [4] get much attention because of its outstanding energy density (0.15-0.2 kWh kg^{-1}) while supercapacitors (SCs) [5] stand out owing to its remarkable power density (2-5 kW kg^{-1}) and stable cyclic ability (over 100000 times). Nowadays, the LIBs and SCs are widely applied in manufacturing industry, hybrid electrical vehicle, smart power grids and so on. However, the low power density and poor cyclic stability of LIBs and low energy density of SCs cannot meet the higher and higher demand of people. Therefore, many researchers turn their view to develop a new energy storage system with both outstanding energy density and power density.

Lithium ion capacitors (LICs) are born at this moment by combining a battery-type anode and a capacitor-type cathode [6-8]. To date, a few LICs have been reported containing a wide work voltage window, fast charge/discharge process and superior cycling life. Nevertheless, the existing LICs have an obvious imbalance between two electrodes, resulting from its capacitive reaction that cathode is faster than the intercalation reactions of anode. Therefore, it is of importance to choose proper anode materials with great rate capability to improve this imbalance for a high-performance LICs [9]. Among anode materials, MnO_2 exhibits a low cost and excellent electrochemical properties, gradually becoming a substitute of expensive rare metal oxides. For example, Liu et al. developed bowl-like MnO_2 nanosheets presenting a specific capacitance of 379 F g^{-1} at a current density of 0.5 A g^{-1} while the capacitance retained ratio of 60.5% from 0.5 to 10 A g^{-1} and after 5000 times the capacitance can maintain 87.3% of the original value [10]. Besides, Won-Sub Yoon et al. reported a l-MnO_2 3D nanoarchitecture for LIBs with high capacities of ~1400 mAh g^{-1} at 100 mA g^{-1} and ~749 mAh g^{-1} at 1000 mA g^{-1} [11]. Based on this excellent rate capability, MnO_2 can effectively balance the kinetics of cation and anion, which is helpful to assemble a high-performance LICs.

Carbon materials (such as AC, CNT, graphene, etc) are widely selected as lithium ion supercapacitor electrodes because of their stable and devisable structure, superior conductive characteristic and economic practicality [12, 13]. The wide application in both LIBs and SCs attracts a lot of attention of researchers. For a more excellent electrode, many workers put in a lot of effort to optimize the carbonaceous materials. For example, Huang et al. used F-GDY as anode with a great rate performance (1825.9

mAh g^{-1} at 0.1 A g^{-1}, 979.2 mAh g^{-1} at 5 A g^{-1}) [14]. Peng et al. reported a CNT-threaded N-doped carbon film (CNCF), showing a remarkable specific capacitance of 340 F g^{-1} at 2 A g^{-1}, long cycling life with a Coulombic efficiency of 97.7% after 10000 times at 20000 mA g^{-1} as a supercapacitor electrode [15]. Inspired by these work, N-doped porous carbons are a kind of vital material as the capacitor-type cathode for a more glorious lithium ion capacitor.

Here, we synthesized a kind of MnO_2 nanowire via a simple one spot hydrothermal method. As an anode of LICs, MnO_2 nanowire displays a capacity of 185 mAh g^{-1}at 200 mA g^{-1} with 41.1 % capacity retention at 5C, which benefits from the 3D stacked nanostructure MnO_2 NWs exposing more active sites, increasing surface area and improving the kinetics of Li ions (Li^+). This brilliant rate capacity is beneficial for balancing kinetics between anode and cathode. Particularly, we designed a non-aqueous LICs with a MnO_2 nanowires as anode and an NPC material as cathode. This N-doped 3D porous carbon increases the specific surface area, offering more adsorption sites to shorten the ion transport pathway. The N doping optimizes the wettability between porous carbon cathode and the electrolyte. Therefore, the MnO_2//NPC LIC can deliver a fine capacity of 150 mAh g^{-1} at 500 mAh g^{-1}. Moreover, it demonstrates a superior energy density of 82.7 Wh kg^{-1} at power density of 1050 W kg^{-1} with a good cycling life of LIC with a 20% retention after 1000 times. Especially, a red LED was powered by this MnO_2//NPC LIC, which proved its excellent practical potential.

2. Experimental Section

2.1. Preparation of MnO_2 NWs

The MnO_2 NWs were prepared via the one-step hydrothermal method [16]. Firstly, 158.3 mg $KMnO_4$ and 53.5 mg NH_4Cl were separately added to 30 mL of deionized (DI) water and stirred with a duration of 15 min. After that, the mixture was stirred for 20 min and then dumped into a 100 mL autoclave at 200 °C for 24 h. After cooling down to ambient temperature, the sample was obtained by centrifuge and wash using DI and ethanol 3 times. Finally, the MnO_2 NWs was obtained after drying at 60 °C for 24 h in an oven.

2.2. Preparation of NPC

NPC was synthesized as previously reported [17]. Briefly, gelatin, citric acid and $FeCl_3$ (mass ratio 3:1:4) were added in 0.03 L DI at 90 °C until dissolved. Then, the dried brown gel was calcined at a two-step process (300 °C for 60 min with 3 °C min^{-1}, 800 °C for 120 min at 5 °C min^{-1}) under an Ar/H_2 atmosphere. After acid and DI washing, the black power was obtained. Finally, the power and KOH (mass ratio: 1:3) were mixed homogeneously and activated at 650 °C for 2h. After further acid and DI washing, the NPC was prepared in an oven at 60 °C.

2.3. Electrode Preparation

The anode was prepared by mixing MnO_2 NWs, acetylene black and poly(vinylidene fluoride) (PVDF) with a weight ratio of 7:2:1 in N-Methyl pyrrolidone (NMP). Then, the slurry was smeared on the Cu foil. Similarly, this cathode was synthesized containing N doped porous carbon, acetylene black and PVDF with the same ratio coated on an aluminum foil. All of the prepared electrodes were dried under 100 °C for 12 h in a vacuum oven. These half cells (2032 coin-type cell) were assembled with lithium metal as counter electrode and reference electrode as well as commercial LBC3008A as the electrolyte in the Ar-filled glove box. Before composing the LICs, we gave MnO_2 NWs anodes in close contact with Li metal in the commercial electrolyte LBC3008A for 48 h for a prelithium process. The anode and cathode mass ratio were about 1:3. Specific capacity of MnO_2 NWs//NPC LIC was calculated on a base of anode mass.

2.4. Characterizations

The XRD test was measured on a Rigaku P/max 2200VPC with Cu Kα radiation to investigate the phase of MnO_2 NWs and NPC. SEM (XL 30 ESEM-FEG, FEI Company) and TEM was performed to characterize the surface and interior porous features of as-prepared products. Cyclic voltammetry (CV) and electricimpedance spectroscopy (EIS) were executed on a CHI660E electrochemical workstation (Chenhua, Shanghai). Here, EIS was measured between 10^{-2} Hz and 10^5 Hz. Cycling and rate measurements were carried out by a LAND CT2001A battery measurement system.

The energy density and power density were calculated as follow [18]:

$$P=\Delta V\times i/m \quad (1)$$

$$E=P\times t/3600 \quad (2)$$

$$\Delta V=(V_{max}+V_{min})/2 \quad (3)$$

3. Results and discussion

3.1. MnO_2 NWs as the anode

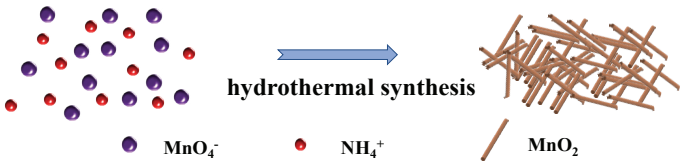

Figure 1. The schematic diagram of MnO_2 nanowires.

The MnO_2 NWs were prepared via a simple hydrothermal process in Figure 1. $KMnO_4$ as Mn source was reduced from Mn (VII) to Mn (IV) to form a stable MnO_2 NWs. Following is the chemical reaction:

$$2NH_4MnO_4 \rightarrow N_2\uparrow+2MnO_2+4H_2O+O_2\uparrow$$

The nanostructure MnO_2 possesses large surface area and more electrochemical sites, and hence optimize the kinetics of Li^+. [19] From SEM images in Figure 2a, MnO_2 exhibits nanowire morphology. Many MnO_2 NWs are intertwined presenting a three-dimensional (3D) network. From a magnification SEM image in Figure 2b, the length of MnO_2 NWs is about 500 ~ 700 nm with a diameter of about 50 nm. Moreover, XRD analysis was conducted to get a further crystal phase of MnO_2 NWs in Figure 2c. It shows that the obtained MnO_2 nanowires are well consistent with the pure MnO_2 with a space group of I4/m (87) (JCPDS: 44-0141). Moreover, the diffraction peaks at 12.8°, 18.1°, 28.8°, 36.7°, 37.5°, 39.0°, 42.0°, 49.9°, 56.4°, 60.3°, 65.1°, and 69.7° correspond to the (110), (200), (310), (400), (211), (330), (301), (411), (600), (521), (002) and (541) planes, respectively, which further confirms the successful preparation of a high crystal pure phase MnO_2 NWs.

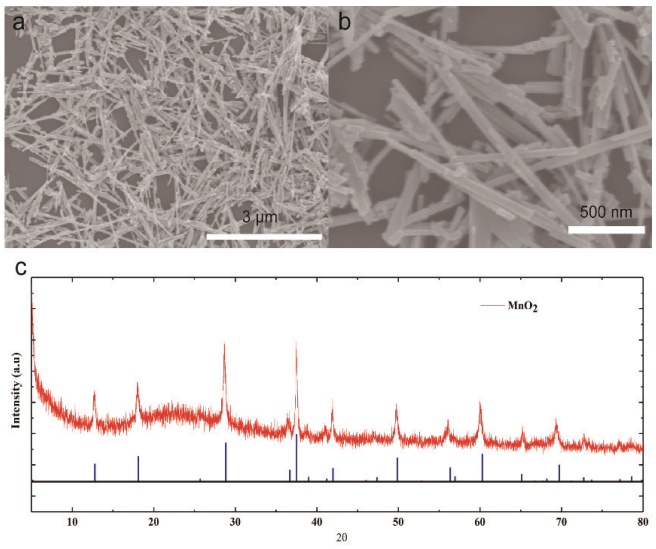

Figure 2. (a) SEM image of MnO_2 NWs with a scale of 3 μm. (b) Magnified SEM image with a scale of 500 nm. (c) XRD pattern of MnO_2 NWs, which confirms that high crystal pure phase 3D stacked MnO_2 NWs are synthesized.

In order to study the electrochemical performance of MnO_2 NWs as anode in LICs, half cells with a counter electrode of Li foil between 0.01 and 3 V (vs. Li/Li^+) was tested. In Figure 3a, CV curves of MnO_2 electrodes at a series of scan rates between 0.1-0.5 mV s^{-1} are presented to reflect the Li^+ transfer in/out of the MnO_2 NWs. At a scan rate of 0.1 mV s^{-1}, the reduction peak at about 0.45 V is assigned to the SEI formation and the transform from Mn (IV) to Mn (0). The oxidation peak at about 1.3 V is attributed to the reoxidation from Mn (0) to Mn (IV). The other CV curves display a similar reaction mechanism. The charge/discharge curves in Figure 3b also proves this process. The reaction is summarized as follow:[20]

$$MnO_2+4Li \leftrightarrow 2Li_2O+Mn$$

Moreover, the CV curves at other scan rates exhibit similar redox peaks and retain the curve shape, exhibiting that the MnO_2 NWs have a satisfied rate capacity. Especially, the excellent rate properties are proved from Figure 3c. When the current density is 0.2, 0.4, 0.6, 0.8, 1 and 2 A g^{-1}, the sample shows stable capacities of 185, 175, 122, 100, 76 and 25 mAh g^{-1}. That is to say, when the current density increases 5 times, the capacity retention reaches 41.1%. More importantly, the MnO_2 NWs anode remains 170 mAh g^{-1} after 1000 cycles in Figure 3e, displaying the fine long cyclic stability. The EIS result is conducted in Figure 3d. As known, the smaller the diameter of this semicircle is, the faster the charge transfer. A small charge transfer resistance of MnO_2 NWs benefits to the fast insertion and de-intercalation of Li^+. These outstanding performances are attributed to the nanostructure of MnO_2 and the exposed active sites, which makes MnO_2 NWs a proper candidate for LICs anode.

3.2. NPC as the cathode

N-doped hierarchical porous carbon was chosen as cathode for the LICs. In Figure 4a, a bulk carbon material with a macropore structure is observed. The surface macropores are distributed uniformly with about 500 nm in diameter. The TEM image in Figure 4b exhibits willow-leaf-shaped mesopores. These special pores show a ~160 nm long and a ~40 nm wide. This particular porous structure will effectively shorten transfer pathway and accelerate the transfer of the electrolyte ion. In Figure 4c, the XRD pattern of NPC reflects the degree of graphitization. The peaks at about 25° and 44° are attributed to (002) and (100) planes and this wide shape demonstrates the amorphous nature. This defective structure is resulted from the N and O atom defects reported in previous work. Moreover, the N-doping improves the contact of electrode and electrolyte, further enhancing the electrochemical activation of NPC as cathode for LICs.[21]

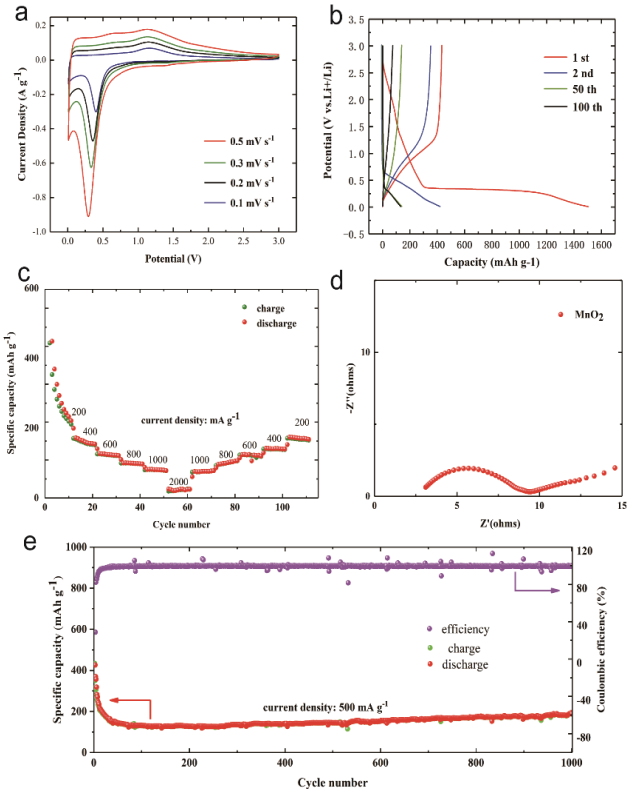

Figure 3. The Li^+ storage properties of MnO_2 NWs anode: (a) CV curves of MnO_2 NWs with scan rates from 0.1 to 0.5 mV s^{-1}, (b) The selected charge-discharge curves at 500 mA g^{-1}, (c) The rate properties with current densities between 200-2000 mA g^{-1}, (d) EIS spectroscopy between 0.01 and 10^5 Hz, (e) the long cycling property and Coulombic efficiencies of this sample at 500 mA g^{-1}, displaying a satisfied electrochemical performance.

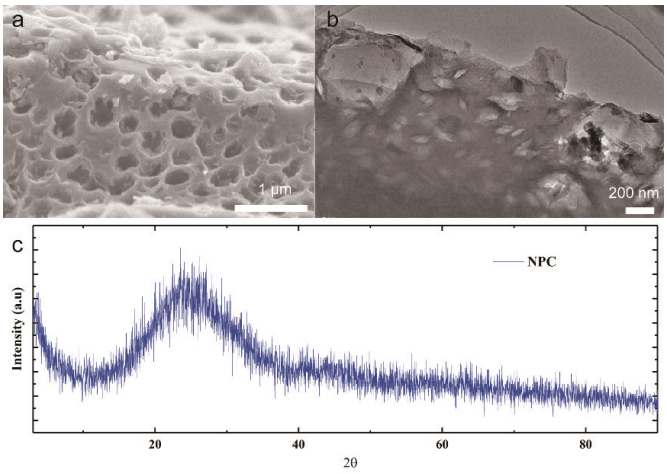

Figure 4. (a) SEM image of NPC at 1μm, (b) TEM image of NPC at 200 nm, (c) XRD pattern of NPC, which shows that N-doped porous carbon possesses a meso and macro structure.

The electrochemical property of nitrogen doped hierarchical porous carbon materials was studied in Figure 5. The CV curve at 1mV s^{-1} with an extended potential window of 2-4.2 V was shown in Figure 5a. Non-redox peaks in these rectangles reflect an ideal capacitive contribution, which corresponds to the charge/discharge curve without any platform in Figure 5b. The selected curves of the 1st, 2nd, 50th and 100th cycles overlap well with each other, illustrating that the NPC cathode has the super stable adsorption ability at 0.5 A g^{-1}. Moreover, the rate property test of NPC cathode in Figure 5c give a series capacity of 97, 75, 66 and 60 mAh g^{-1} at 200, 600, 1000 and 2000 mA g^{-1}, respectively. EIS test in Figure 5d shows that the NPC cathode has a small charge transfer resistance and ion diffusion resistance, further presenting a candidate with a fast ion storage. The cycling performance of NPC in Figure 5e illustrates that the capacity of NPC cathode remains about 30 mAh g^{-1} after 700 cycles. This good adsorption ability is attributed that the 3D porous structure increases the specific surface area, offers more adsorption sites and shortens the ion transport pathway. The N doping optimizes the wettability between NPC cathode and the electrolyte, much suitable for a satisfied performance LIC.

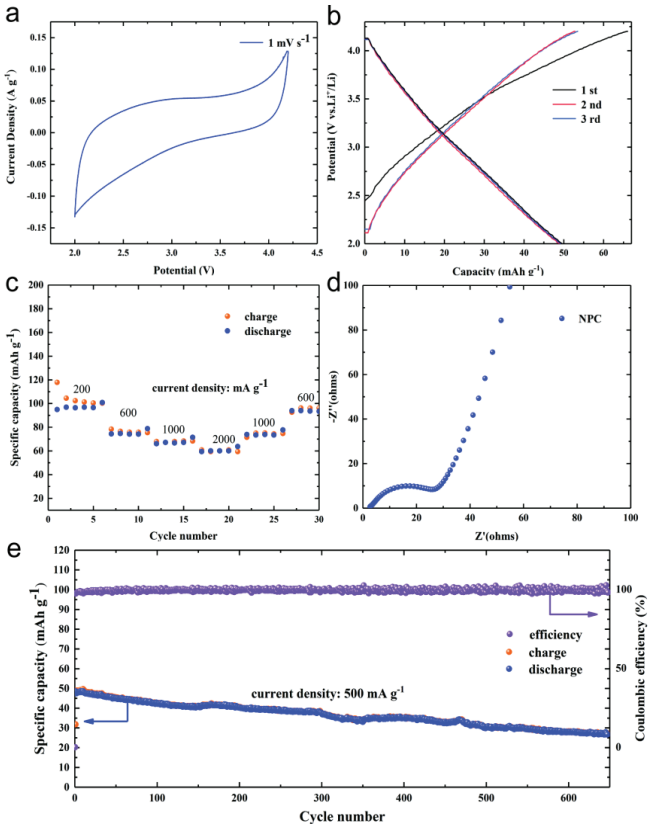

Figure 5. The PF_6^- absorption ability of the NPC cathode: (a) the CV curves of NPC at 1 mV s^{-1}, (b) The charge/discharge curves at the 1st, 2nd, 50th and 100th cycle at 500 mA g^{-1}, (c) The rate property of NPC at 200, 600, 1000, 2000 mA g^{-1}, (d) The EIS spectrum of NPC between 0.01 and 10^5 Hz, (e) The cycling life of NPC at 500 mA g^{-1}, displaying superior adsorption ability.

3.3. MnO_2 NWs//NPC LICs

Utilizing the prepared prelithiated MnO_2 nanowires as anode and the NPC we previously reported as cathode, a LICs with a commercial electrolyte of LBC3008A was assembled. The whole charge/discharge process is explained in detail from Figure 6. In a charge process, the NPC cathode adsorbs the PF_6^- in the surface macro and meso pores with N-doping defects. At the same time, the Li^+ is transferred and reacts to the MnO_2 nanowires anode. The discharge process is the opposite of the charge process. In order to balance the anode and cathode, we make a mass ratio of anode and cathode be 1:3 according to the literature. Moreover, the 3D network of stacked MnO_2 nanowires offers more reaction sites for a fast Li^+ migration, effectively offsetting the intrinsic slow migration rate of Li^+. The 3D porous structure offers more adsorption sites and the N doping optimizes the wettability of NPC. Both of these two advantages make MnO_2 nanowires anode and NPC cathode more matched to construct MnO_2//NPC LICs.

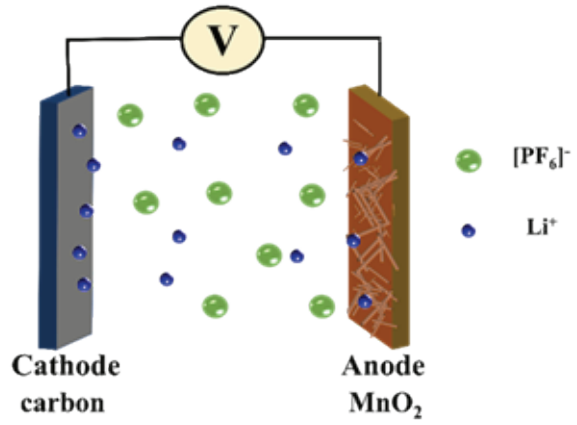

Figure 6. The Schematic model of the LICs assembled by MnO_2 nanowires as anode and NPC as cathode, accuratly interpreting the charge/discharge mechanism of MnO_2 NWs//NPC LICs.

The electrochemical property of MnO_2//NPC LICs is evaluated in Figure 7. Figure 7a exhibits CV curves at different scan rate with an extended potential window of 0-4.2 V. Similar near rectangles and non-redox peaks display an ideal capacitive contribution, which corresponds to no platform in the charge/discharge curve in Figure 7b. The maintenance of rectangle shape further reflects the high rate performance. The charge and discharge curves of MnO_2//NPC LICs exhibit a capacity of 250, 156 and 100 mAh g^{-1} (on base of anode mass) at 0.2, 0.4, 0.6 A g^{-1}, respectively. Its result also confirms the MnO_2//NPC LICs has a good rate property. More interestingly, the satisfied retention of 20% after 1000 times at 500 mA g^{-1} in Figure 7c, demonstrates a stable performance of the MnO_2//NPC LICs. The energy density of 82.7 Wh kg^{-1} and a remarkable power density of 1.05 kW kg^{-1} is comparable to those aqueous supercapacitors such as LF-P@C//ARGO [22], LMO/AC Li - Ion flow capacitor [23] and so on in Figure 7d. This illuminates the extended potential range can largely improve the energy density of MnO_2//NPC LICs. The success of a lighted red LED (Voltage: 2 V, current range: 5 mA-17.5 mA) (inset Figure 7d) powered by the MnO_2//NPC LICs further proves its excellent practical potential.

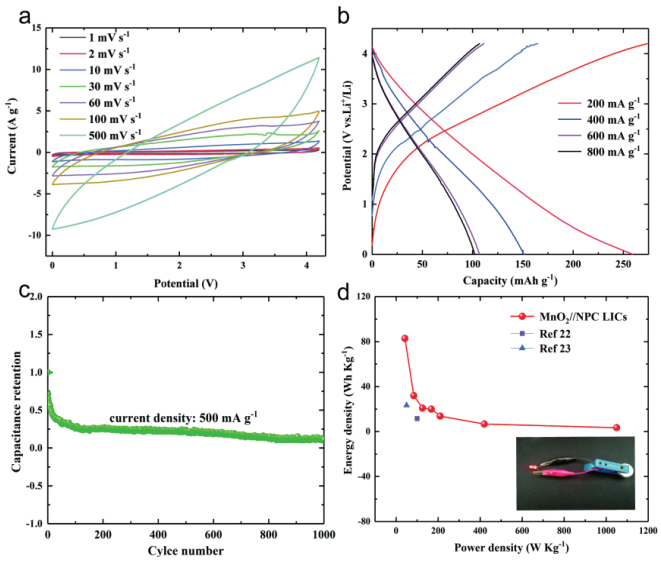

Figure 7. The electrochemical properties of MnO_2 NWs//NPC LICs: (a) The CV curves from 1 mVs^{-1} to 500 mVs^{-1}, (b) The charge/discharge curves at 200, 400, 600 and 800 mA g^{-1}, (c) The cycling stability at 500 mA g^{-1} after 1000 times, (d) The relationship of energy density and power density of MnO_2 NWs//NPC LICs and the comparison with other literatures. The inset is a photo show of a lighted red LED powered by our MnO_2 NWs//NPC LICs.

4. Conclusion

In this paper, the MnO2 nanostructure was successfully prepared via a simple chemical reaction. The obtained MnO2 nanowires expose more active sites and improve the reaction rate with Li+. As an anode of LICs, it delivers a capacity of 185 mAh g-1 at 0.5 A g-1 and accompanies a 41.1 % capacitance maintaining at 1 A g-1. The fine rate performance is beneficial for balancing the kinetics between anode and cathode. Moreover, the NPC material was chosen as cathode to design a non-aqueous LICs. The N-doped 3D porous carbon offers a larger specific surface area, more adsorption sites and a shorter ion transport pathway. The N doping optimizes the wettability between NPC cathode and the electrolyte. In consequence, the MnO2//NPC LICs can display a brilliant capacity of 150 mAh g-1 at 500 mA g-1. Meanwhile, it demonstrates a high energy density of 82.74 Wh kg-1 and a brilliant power density of 1.05 kW kg-1. The success of powering a red LED further proves its excellent practical potential, which provides a realizable thought for the future storage system.

Author Contributions: W.B. Wang, Y.H. Shi, Y. Su, Y.H. Wang and H.Z. Sun are contributors in this work. W.B. Wang performed the whole experiment including samples preparation, electrode preparation, the cell assembly in a glove box and the measurement of electrochemical properties of the cycling and rate performance, the CV curves, the EIS test. Y.H. Shi, Y. Su and Y.H. Wang helped to characterize the morphology features such as SEM, TEM and XRD measurements and analyse the obtained results. Professor H.Z. Sun conducted this whole paper.

Conflict of Interest: No conflict of interest was reported by the authors.

Acknowledgments: Financial supports from the NSFC (21574018, and 51433003), Jilin Provincial Education Department (543), Jilin Provincial Key Laboratory of Advanced Energy Materials (Northeast Normal University) are gratefully acknowledged.

References

[1] Y Wang, S Su, L Cai, et al. Monolithic integration of all-in-one supercapacitor for 3D electronics. Advanced Energy Materials 2019; 9(15): 1900037.

[2] Q Zeng, X Zhang, X Feng, et al. Polymer-passivated inorganic cesium lead mixed-halide perovskites for stable and efficient solar cells with high open-circuit voltage over 1.3 V. Advanced Materials 2018; 30(9): 1705393.

[3] J Guo, F Wan, X Wu, et al. Sodium-ion batteries: work mechanism and the research progress of key electrode materials Journal of Molecular Science. 2016; 32(04): 265-279.

[4] D Xu, W Liu, C Zhang, et al. Monodispersed FeCO3 nanorods anchored on reduced graphene oxide as mesoporous composite anode for high-performance lithium-ion batteries. Journal of Power Sources 2017; 364: 359-366.

[5] K Yang, K Cho, S Yang, et al. A laterally designed all-in-one energy device using a thermoelectric generator-coupled micro su-percapacitor, Nano Energy 2019; 60: 667-672.

[6] J M Campillo-Robles, X Artetxe, K del Teso Sanchez, et al. General hybrid asymmetric capacitor model: Validation with a com-mercial lithium ion capacitor. Journal of Power Sources 2019; 425: 110-120.

[7] C Li, S Cong, Z Tian, et al. Flexible perovskite solar cell-driven photo-rechargeable lithium-ion capacitor for self-powered wearable strain sensors. Nano Energy 2019; 60: 247-256.

[8] C Liu, QQ Ren, SW Zhang, et al. High energy and power lithium-ion capacitors based on Mn3O4/3D-graphene as anode and activated polyaniline-derived carbon nanorods as cathode. Chemical Engineering Journal 2019; 370: 1485-1492.

[9] H Wang, C Zhu, D Chao, et al. Nonaqueous hybrid lithium-ion and sodium-ion capacitors. Advanced Materials 2017; 29(46): 1702093.

[10] P Liu, Y Zhu, X Gao, et al. Rational construction of bowl-like MnO2 nanosheets with excellent electrochemical performance for supercapacitor electrodes. Chemical Engineering Journal 2018; 350: 79-88.

[11] H Kim, N Venugopal, J Yoon, et al. A facile and surfactant-free synthesis of porous hollow □-MnO2 3D nanoarchitectures for lithium ion batteries with superior performance. Journal of Alloys and Compounds 2019; 778: 37-46.

[12] C Yang, M Zhang, N Kong, et al. Self-supported carbon nanofiber films with high-level nitrogen and phosphorus co-doping for advanced lithium-ion and sodium-ion capacitors, Acs Sustainable Chemistry & Engineering 2019 7(10): 9291-9300.

[13] L Zhang, Y Wang, Z Niu, et al. Single atoms on graphene for energy storage and conversion. Small Methods 1800443.

[14] X Shen, J He, K Wang, et al. Fluorine-enriched graphdiyne as an efficient anode in Lithium-ion capacitors. ChemSusChem 2019; 12(7): 1342-1348.

[15] Y Liu, G Li, Z Chen, et al. CNT-threaded N-doped porous carbon film as binder-free electrode for high-capacity supercapacitor and Li-S battery. Journal of Materials Chem-

istry A 2017; 5(20): 9775-9784.
[16] S Wang, BY Guan, L Yu, et al. Rational design of three-layered TiO2@Carbon@MoS2 hierarchical nanotubes for enhanced lithium storage. Advanced Materials 2017; 29(37): 1702724.
[17] Y Shi, L Zhang, TB Schon, et al. Porous carbon with willow-leaf-shaped pores for high-performance supercapacitors. Acs Ap-plied Materials & Interfaces 2017; 9(49): 42699-42707.
[18] Q Xia, H Yang, M Wang, et al. High dnergy and high power lithium-ion capacitors based on boron and nitrogen dual-doped 3D carbon nanofibers as Both cathode and anode. Advanced Energy Materials 2017; 7(22): 1701336.
[19] Z-H Huang, Y Song, DY Feng, et al. High Mass Loading MnO2 with Hierarchical Nanostructures for Supercapacitors. ACS Nano 2018; 12(4): 3557-3567.
[20] L Feng, Z Xuan, H Zhao, et al. MnO2 prepared by hydrothermal method and electrochemical performance as anode for lithi-um-ion battery. Nanoscale Research Letters 2014; 9: 290.
[21] S Wang, Y Shi, C Fan, et al. Layered g-C3N4@Reduced Graphene Oxide Composites as Anodes with Improved Rate Perfor-mance for Lithium-Ion Batteries. Acs Applied Materials & Interfaces 2018; 10(36): 30330-30336.
[22] H Gao, J Wang, R Zhang, et al. An aqueous hybrid lithium ion capacitor based on activated graphene and modified LiFePO4 with high specific capacitance. Materials Research Express 2019; 6(4): 045509.
[23] H Liu, L Liao, YC Lu, et al. High energy density aqueous li-ion flow capacitor. Advanced Energy Materials 2017; 7(1): 1601248.